THE JOURNAL OF BIOLOGICAL CHEMISTRY
Vol. 271, No. 23, Issue of June 7, pp. 13804–13810, 1996
© 1996 by The American Society for Biochemistry and Molecular Biology, Inc.
Printed in U.S.A.

Identification of Three Subunits of the High Affinity ω-Conotoxin MVIIC-sensitive Ca^{2+} Channel*

(Received for publication, December 6, 1995, and in revised form, February 20, 1996)

Hongyan Liu‡§¶, Michel De Waard§, Victoria E. S. Scott§, Christina A. Gurnett§¶, Vanda A. Lennon‖, and Kevin P. Campbell§‡‡**

From the §Howard Hughes Medical Institute, Department of Physiology and Biophysics, ‡Program in Neuroscience, University of Iowa College of Medicine, Iowa City, Iowa 52242 and ‖Neuroimmunology Laboratory, Departments of Immunology and Neurology, Mayo Clinic, Rochester, Minnesota 55905

N-, P- and Q-type voltage-dependent Ca^{2+} channels control neurotransmitter release in the nervous system and are blocked by ω-conotoxin MVIIC. In this study, both a high affinity and a low affinity binding site for ω-conotoxin MVIIC were detected in rabbit brain. The low affinity binding site is shown to be present on the N-type Ca^{2+} channel. Using optimized conditions for specific labeling of the high affinity ω-conotoxin MVIIC receptor and a panel of subunit specific antibodies, the molecular structure of the high affinity receptor was investigated. We demonstrate for the first time that this receptor is composed of at least α_{1A}, $\alpha_2\delta$, and any one of the four brain β subunits. Such association of different β subunits with α_{1A} and $\alpha_2\delta$ components may produce Ca^{2+} channels with distinct functional properties, such as P- and Q-type.

Voltage-dependent Ca^{2+} channels play a central role in neurotransmitter release and muscle contraction. Several voltage-dependent Ca^{2+} channels have been identified which are classified by electrophysiological and pharmacological criteria as T-, L-, N-, P-, and Q-type Ca^{2+} channels (1, 2). To date, three different types of these Ca^{2+} channels (N-, P-, and Q-type) are known to mediate synaptic transmission in the nervous system (3, 4). Biochemical characterization of the brain N-type Ca^{2+} channel revealed that it is composed of α_{1B}, $\alpha_2\delta$, and β subunits and a unique 95-kDa protein (5, 6). Among the subunits of brain N-type Ca^{2+} channels, α_1 is the pore-forming subunit and the receptor for antagonist drugs (7); β is cytoplasmic and regulates the function of α_1 (8–10); $\alpha_2\delta$ is heavily glycosylated and modifies the functional properties of the channel complex (11, 12). Molecular cloning has thus far identified six different α_1 genes (S, A, B, C, D, and E), four different β genes (1, 2, 3, and 4), and one $\alpha_2\delta$ gene. Several splice isoforms for α_1, β, and $\alpha_2\delta$ genes have also been identified (13–18).

Although P- and Q-type Ca^{2+} channels seem to play an even greater role than N-type channels in neurotransmission, little is known about the structural aspects of these channels (4, 19). Pharmacologically, both channels can be blocked by ω-agatoxin IVA and ω-conotoxin (CTX)[1] MVIIC (20–22), although both have different sensitivities to ω-agatoxin IVA (22). However, it has not been established with certainty whether the P- and Q-type Ca^{2+} channels are encoded by the same α_1 subunit gene; or whether they represent different α_1 gene products (1, 12, 22, 23). Since the activity of α_{1A} subunits expressed in *Xenopus* oocytes can be blocked by both ω-agatoxin IVA and ω-CTX MVIIC, it has been proposed that this subunit may be the pore-forming subunit of P- and/or Q-type Ca^{2+} channels (1, 23). Lack of specific blockers to distinguish P- and Q-type channels has made it difficult to further characterize these channels by either electrophysiological or biochemical approaches.

The major types of Ca^{2+} channels controlling neurotransmission (N-, P-, and Q-type) have been shown to be blocked by ω-CTX MVIIC (24, 25). In this study, we identified a high affinity ω-CTX MVIIC receptor which can be distinguished from the low affinity N-type Ca^{2+} channel. Our data demonstrate for the first time that the high affinity ω-CTX MVIIC receptor is composed of at least an α_{1A}, $\alpha_2\delta$, and any one of the four different brain β subunits. The association of different β subunits with the α_{1A} subunit supports a structural heterogeneity of Ca^{2+} channels which may be the basis for functional differences observed between P- and Q-type channels.

EXPERIMENTAL PROCEDURES

Materials—^{125}I-ω-Conotoxin (ω-CgTX) GVIA and ECL immunoblotting kit were from Amersham Corp., ^{125}I-ω-CTX MVIIC from DuPont NEN, ω-CgTX GVIA from Bachem, protein G-Sepharose from Pharmacia Biotech Inc., TNT coupled reticulocyte lysate system from Promega, Hydrazide Avidgel from Unisyn Technologies, ω-CTX MVIIC was a kind gift from Neurex Corporation. All chemicals are of reagent grade.

Ligand Binding Analysis of the ω-CTX MVIIC Receptor and the N-type Ca^{2+} Channel—Rabbit brain membranes were prepared as detailed elsewhere (26). Protein concentration was determined by the method of Lowry (27). To obtain enough material of ^{125}I-ω-CTX MVIIC, ^{125}I-ω-CTX MVIIC (specific activity, 2200 Ci/mmol) was mixed with unlabeled ω-CTX MVIIC to reach a specific activity of 440 Ci/mmol. Aliquots (50 μg of protein) of membranes were incubated with increasing concentrations (0.05–8 nM) of ^{125}I-ω-CTX MVIIC at 25 °C for 1 h in a total volume of 200 μl of buffer A (10 mM HEPES, pH 7.4, 0.2 mg/ml bovine serum albumin, 100 mM NaCl, 0.75 mM benzamidine, 0.1 mM phenylmethylsulfonyl fluoride) containing 0.1 mM EDTA, and 0.1 mM EGTA. The receptor-ligand complexes were collected on GF/B filters and washed rapidly with 4 ml of ice-cold buffer A. The counts remaining on the filter represent total binding. Nonspecific binding was determined by the addition of 0.5 μM nonradioactive ligand prior to the addition of radioactive ligand. Specific binding was calculated by sub-

* The costs of publication of this article were defrayed in part by the payment of page charges. This article must therefore be hereby marked "*advertisement*" in accordance with 18 U.S.C. Section 1734 solely to indicate this fact.

¶ Supported by American Heart Association-Iowa Affiliate Predoctoral Fellowship.

** Supported by National Institutes of Health, NCI Grant CA-37343.

‡‡ An Investigator of the Howard Hughes Medical Institute. To whom correspondence should be addressed: Howard Hughes Medical Institute, University of Iowa College of Medicine, 400 EMRB, Iowa City, IA 52242. Tel.: 319-335-7867; Fax: 319-335-6957; E-mail: kevin-campbell@uiowa.edu; WWW address: http://www-camlab.physlog.uiowa.edu/home.htm.

[1] The abbreviations used are: CTX, conotoxin; ω-CgTX GVIA, ω-conotoxin GVIA; ω-CTX MVIIC, ω-conotoxin MVIIC; PCR, polymerase chain reaction; FP, fusion protein; GST, glutathione *S*-transferase; mAb, monoclonal antibody.

tracting nonspecific binding from total binding. ^{125}I-ω-CgTX GVIA binding was assayed similarly to ^{125}I-ω-CTX MVIIC but without EGTA and EDTA in buffer A. Binding of ^{125}I-ω-CTX MVIIC and ^{125}I-ω-CgTX GVIA to the solubilized membrane extracts are the same as described above. All binding data were analyzed with Grafit software (Sigma) and all results were presented as value ± S.E. Each sample point represents the average of triplicates for all binding and immunoprecipitation experiments in this study.

Competition of Unlabeled ω-CTX MVIIC with ^{125}I-ω-CgTX GVIA Binding—Rabbit brain membranes (4 mg/ml) were solubilized for 1 h on ice in buffer (0.5 M NaCl, 1% (w/v) digitonin, 10 mM HEPES, pH 7.4) plus protease inhibitors mixture A (0.6 μg/ml pepstatin A, 0.5 μg/ml aprotinin, 0.5 μg/ml leupeptin, 0.1 mM phenylmethylsulfonyl fluoride, 0.75 mM benzamidine). Nonsolubilized material was sedimented by centrifugation in a Beckman TL 100 for 10 min at 400,000 × *g*. The supernatant was diluted 8-fold with buffer (10 mM HEPES, pH 7.4, 0.1 mM EDTA, 0.1 mM EGTA, 0.5 μg/ml aprotinin, 0.5 μg/ml leupeptin). Aliquots were mixed with increasing concentrations (0.001 nM to 1 μM) of ω-CTX MVIIC for 10 min before addition of ^{125}I-ω-CgTX GVIA (42.5 pM). After incubating for 1 h at room temperature, receptor-ligand complexes were collected on GF/B filters and washed as described above. For binding to brain membranes, 50 μg of brain membranes were incubated with increasing concentrations of ω-CTX MVIIC for 10 min in 200 μl of buffer (10 mM HEPES, pH 7.4, 62.5 mM NaCl, 0.1% (w/v) bovine serum albumin, 0.1 mM EDTA, 0.1 mM EGTA, 0.5 μg/ml aprotinin, 0.5 μg/ml leupeptin) before addition of ^{125}I-ω-CgTX GVIA (0.1 nM). The IC_{50} was determined by Grafit software using the average of triplicates. Since the concentration of ^{125}I-ω-CgTX GVIA used should not affect the presentation of IC_{50} in the competition curve, data were normalized by setting ^{125}I-ω-CgTX GVIA binding in the absence of ω-CTX MVIIC as 100%.

Primers Used in Polymerase Chain Reaction (PCR) for Production of Fusion Proteins—α_{1A} forward 5′-CCTTGGATCCCGAGATGCGGAAACAGA-3′ (2633–2806 of GenBank™ accession no. X57476), α_{1A} reverse 5′-CCTTGAATTCCTTTCGGCCTTGTCGTC-3′ (3070–3201); α_{1C} forward 5′-GGAAGGATCCGAGCGAAAGAAGCTGGC-3′ (3064–3090 of GenBank™ no. M67516), α_{1C} reverse 5′-AGGTGAATTCGGCCCACAGGCATCTCG-3′ (3307–3333); 2Tβ_2 primers: rat 2Tβ_2 forward 5′-TCGGATCCGAAGAAGAACCTTGTCTGG-3′ (1759–1777 of GenBank™ no. M80545); rat 2Tβ_2 reverse 5′-TCGAATTCAGTAGCGATCCTTAGATTTATGC-3′ (2087–2110); β_4 primers: rat β_4 *Bam*HI-5′-TTGGATCCACAGCTCTCTCACCGTATCC-3′ (1457–1479 in rat β_4 GenBank™ no. L02315) and rat β_4 *Xba*I- 5′-GGCCGTCTAGAGCCTATGTCGGGAGTCATGGC-3′ (1737–1760).

Preparation of Glutathione S-transferase (GST) Fusion Proteins—pGEX vectors were used to produce rabbit α_{1A} and α_{1C}, rat β_{1b}, β_2, β_3, and β_4 GST fusion proteins. The II-III loop region of rabbit α_{1A} cDNA was amplified with α_{1A} primers. The resulting products were cut with *Bam*HI and *Eco*R I and ligated into a pGEX 1 vector which had been linearized with *Bam*HI and *Eco*R I. The II-III loop region of rabbit α_{1C} cDNA (GenBank™ accession no. X15539) was amplified with α_{1C} primers. The resulting PCR products were cut with *Bam*HI and *Eco*R I and ligated into linearized pGEX 2T. pBluescript rat β_{1b} plasmid was cut at *Nco*I and *Hin*dIII restriction enzyme sites. The fragment containing nucleotide 1343–1987 was isolated and ligated into a pGEX KG vector which had also been linearized with *Nco*I and *Hin*dIII. PCR products were obtained from rat PC12 cDNA with 2Tβ_2 primers. The PCR products were cut with *Bam*HI and *Eco*R I and ligated into a linearized pGEX 2T vector. The C-terminal region of β_4 cDNA was amplified from β_4 cDNA plasmid with β_4 primers. The resulting PCR products were cut with *Bam*HI and *Xba*I and ligated into linearized pGEX KG vector. β_3 GST fusion protein was prepared as detailed elsewhere (28). Each fusion protein construct was sequenced to verify the correct insertion and each fusion protein was purified as described previously (28).

Production of Antibodies against GST Fusion Proteins—250–400 μg of purified GST fusion proteins were emulsified in 1 ml of Freund's complete (initial injection) or incomplete adjuvant (subsequent injections), and injected into multiple subcutaneous sites on New Zealand White rabbits at 2-week intervals. Antisera were collected after the second injection and tested for reactivity with the antigen on immunoblots of GST fusion proteins. Listed here are the injected animals and their immunogen: rabbit 141 and 142 (fusion protein (FP) β_1), rabbit 143 and 144 (FP β_2), rabbit 145 and 146 (FP β_4), sheep 49 (FP β_3), sheep 37 (FP α_{1A}), and sheep 41 (FP α_{IC}). The monoclonal anti-α_{1B} IgG (41) was secreted by a hybridoma produced from the lymph node B cells of a rat hyperimmunized with FP α_{1B} (28). α_{1S} and $\alpha_2\delta$ antibodies are as described elsewhere (26, 29)

Immunoblot Analysis—Fusion proteins or rabbit brain proteins (20–100 μg of protein/lane) were resolved on 3–12% gradient SDS-polyacrylamide gels and transferred to nitrocellulose. Horseradish peroxidase colorimetric detection was performed as described previously (6). An ECL detection system (Amersham Corp.) was used according to the manufacturer's instructions. The β_2 subunit was detected with an ECL immunoblotting technique; all others used horseradish peroxidase colorimetric detection. Since polyclonal antibodies vary in their affinities for different epitopes, immunoblot staining does not necessarily reflect the level of different proteins in a quantitative way.

Immunoprecipitation of ^{35}S-Labeled Full-length β Subunits—The full-length β_{1b}, β_2, β_3, and β_4 subunits were *in vitro* translated using a coupled transcription and translation system (Promega) as detailed elsewhere (30). Immunoprecipitation conditions were intended to be identical to the immunoprecipitation conditions used for native Ca^{2+} channels as described in the following section. Brain membranes (4 mg/ml) were solubilized and diluted as indicated under "Competition of Unlabeled ω-CTX MVIIC with ^{125}I-ω-CgTX GVIA Binding." Triplicates of 25 μl of each β subunit antibody and control α_{1C} antibody were coupled to protein G-Sepharose beads by overnight incubation in phosphate buffered saline. Subsequently, these antibodies were washed with phosphate-buffered saline extensively and incubated with aliquots of solubilized brain extract (1 ml) in buffer (0.1% digitonin, 10 mM HEPES, pH 7.4, 100 mM NaCl, 0.5 μg/ml aprotinin, 0.5 μg/ml leupeptin) for 15 min before the addition of 200,000 cpm of ^{35}S-labeled full-length β subunit per tube for overnight incubation at 4 °C. The antibody-protein G beads were washed extensively with phosphate-buffered saline and subjected to scintillation counting. The nonspecific binding determined from the control α_{1C} antibody was subtracted from the total binding for each antibody to obtain specific binding. Data were presented as values ± S.E.

Immunoprecipitation of Various Types of Ca^{2+} Channels—Brain membranes (4 mg/ml) were solubilized and diluted as described above. The solubilized protein was labeled with 45 pM ^{125}I-ω-CTX MVIIC for 1 h at room temperature. Then aliquots of the labeled extract (0.5–1 ml) were incubated for 3 h with 50 μl of antibody-protein G-Sepharose beads. The beads were quickly washed with 1.5 ml of ice-cold buffer A twice, and total binding was quantified by γ counting. Nonspecific binding was determined by the addition of 0.5 μM unlabeled ω-CTX MVIIC prior to the addition of the labeled toxin. Immunoprecipitation of L-type Ca^{2+} channel was as described elsewhere (26). Saturating immunoprecipitation was achieved with 50 μl of antibody/tube as compared with that of 100 and 150 μl of antibody.

Enrichment of the High Affinity ω-CTX MVIIC Receptor—Affinity-purified sheep 37 (α_{1A}) antibody was coupled to Hydrazide Avidgel AX according to the manufacturer's instructions. Protease inhibitors mixture A was present in all buffers during the partial purification. Rabbit brain membranes (1 g) were solubilized in buffer (1% digitonin, 1 M NaCl, 10 mM HEPES, pH 7.4) for 1 h on ice, followed by centrifugation at 140,000 × *g* for 37 min in a Beckman 45 Ti rotor. The solubilized extracts were diluted 3-fold with ice-cold distilled and deionized water and applied to the heparin-agarose column (50 ml). After washing the heparin column extensively with buffer B (10 mM HEPES, pH 7.4, 0.1% digitonin, 100 mM NaCl), the column was eluted with the buffer B containing 0.7 M NaCl. The eluates from the heparin column were applied to the mAb α_{1B} (CC18) column. Then the α_{1A} column was incubated with the void from the α_{1B} column overnight. The column was washed with 50 ml of buffer B containing 0.6 M NaCl followed by 50 ml of buffer B. Then the column was eluted with glycine buffer (50 mM glycine, pH 2.5, 100 mM NaCl, 0.1% digitonin). 125 μl of 2 M Tris (pH 8.0) were added to every milliliter of eluate immediately after the elution. The eluted material was concentrated with Centricon-100 (Amicon) and subjected to SDS-polyacrylamide gel electrophoresis analysis. The protein concentration was determined either by the method of Lowry (27) or a silver binding method by Krystal (31) for measuring nanogram amounts of proteins.

Preparation of Xenopus Oocytes and Injection—Mature *Xenopus* laevis female frogs were purchased from NASCO (Fort Atkinson, WI). Preparation of *Xenopus* oocytes, cRNA synthesis, and cRNA injection into oocytes were as described previously (10). Fifty nanoliters of various *in vitro* transcribed RNA mixtures were injected per oocyte (0.5 μg/μl α_{1A} and 0.5 μg/μl $\alpha_2\delta_b$ together with either 0.1 μg/μl rabbit β_{2a} (16) and 0.1 μg/μl β_3 in the case of a β_{2a}:β_3 ratio of 1:1, or 0.1 μg/μl β_{2a} and 1 μg/μl β_3 in the case of a β_{2a}:β_3 ratio of 1:10). Electrophysiological recording and data analysis were as described previously (10). Briefly, Ba^{2+} currents were recorded by a standard two-microelectrode voltage-clamp technique using a Dagan amplifier (TEV-200). Voltage and current electrodes (0.5–2 megohms) were filled with 3 M KCl. The bath solution was (in mM): 40 $Ba(OH)_2$, 50 NaOH, 2 KCl, 1 niflumic acid, 0.1

EGTA, 5 HEPES, pH 7.4 (methanesulfonic acid). Ba^{2+} currents were induced by 2-s voltage steps from a holding potential of −90 mV to a testing potential of +10 mV. The number of inactivating exponential components was determined by the best fitting of the current trace using pClamp software (Axon Instruments) according to the Chebyshev procedure. The decay of the current was fitted by either one single or the sum of two exponential functions. The equation used for two exponentials is $I_{Total} = i_1 \cdot \exp(-t/\tau_1) + i_2 \cdot \exp(-t/\tau_2) + C$, where i denotes each monoexponential inactivating component with a time constant τ. C is the offset.

RESULTS

Rabbit Brain Expresses a High Affinity ω-CTX MVIIC-sensitive Ca^{2+} Channel—Both a high affinity and a low affinity binding site for ω-CTX MVIIC were detected in rabbit brain (Fig. 1*A*). Curve fitting of the direct binding curve and Scatchard binding analysis (32) reveal a high affinity binding site with a K_d of 0.37 ± 0.09 nM and a B_{max} of 870 ± 92 fmol/mg; and a low affinity binding site with a K_d of 4 ± 2 nM and a B_{max} of 290 ± 110 fmol/mg. It is technically difficult to analyze a low affinity site ($K_{d2} > K_{d1}$) with a smaller binding capacity because the high affinity site always forms more ligand-bound receptor than the low affinity site (32). The characteristics of the high affinity ω-CTX MVIIC binding site are in approximate agreement with previous results reported for rat and human brain membranes (24, 33, 34). In comparison, ^{125}I-ω-conotoxin GVIA (ω-CgTX GVIA), a specific blocker for N-type Ca^{2+} channel, binds to the same rabbit brain membrane with a K_d of 45 ± 6 pM and a B_{max} of 207 ± 14 fmol/mg (Fig. 1*B*). These results demonstrate that the expression level of the high affinity ω-CTX MVIIC receptor is higher than that of N-type Ca^{2+} channel in rabbit brain; while the expression of the low affinity receptor is similar to that of N-type Ca^{2+} channel. In order to further analyze the ω-CTX MVIIC binding receptor, unlabeled ω-CTX MVIIC was used to compete with [^{125}I] ω-CgTX GVIA for binding to rabbit brain membrane and solubilized brain extracts (Fig. 1*C*). The results reveal an IC_{50} of 7.7 ± 0.3 (brain membranes) and 7.9 ± 0.3 nM (solubilized brain extracts) for ω-CTX MVIIC and a K_i of ~4.4 nM. All of these data suggest that ω-CTX MVIIC binds with low affinity (about 4 nM) to the N-type Ca^{2+} channel. Notably, ω-CTX MVIIC up to 1 nM did not significantly inhibit ^{125}I-ω-CgTX GVIA binding to the N-type Ca^{2+} channel, while it starts to bind to the N-type Ca^{2+} channel at higher than 1 nM concentration (Fig. 1*C*). This important property of ω-CTX MVIIC enabled us to distinguish these two binding sites by specifically labeling only the high affinity receptor with these low toxin concentrations (<1 nM).

α_{1A} and Any One of the Four β Subunits Are Components of the High Affinity ω-CTX MVIIC Receptor—A low concentration of ^{125}I-ω-CTX MVIIC (45 pM) was used to specifically label the high affinity ω-CTX MVIIC receptor. Polyclonal α_{1A} subunit antibodies immunoprecipitated 21 fmol of labeled high affinity ω-CTX MVIIC receptor (84% of total labeled receptors) (Fig. 2*A*). In contrast, monoclonal antibodies raised against the α_{1S} subunit (IIC12) and the α_{1B} subunit (CC18) together with a polyclonal antibody against the α_{1C} subunit (sheep 41) did not sediment significant amounts of labeled high affinity ω-CTX MVIIC receptor (less than 5% of total labeled receptors). In control experiments, however, the mAb against α_{1S} (IIC12) immunoprecipitated more than 80% of ^{3}H-PN200–110 binding to the skeletal muscle L-type Ca^{2+} channel (26); the mAb against α_{1B} (CC18) immunoprecipitated more than 80% of brain N-type Ca^{2+} channel; and the polyclonal antibody against α_{1C} (sheep 41) immunoprecipitated 80% of cardiac L-type Ca^{2+} channel (data not shown). These results demonstrate that the α_{1A} subunit is a component of the brain high affinity ω-CTX MVIIC receptor, which is in agreement with the results from rat brain (35). Furthermore, the data confirm that low concentrations of ω-CTX MVIIC specifically label the brain high affinity ω-CTX MVIIC receptor but not the N-type Ca^{2+} channel.

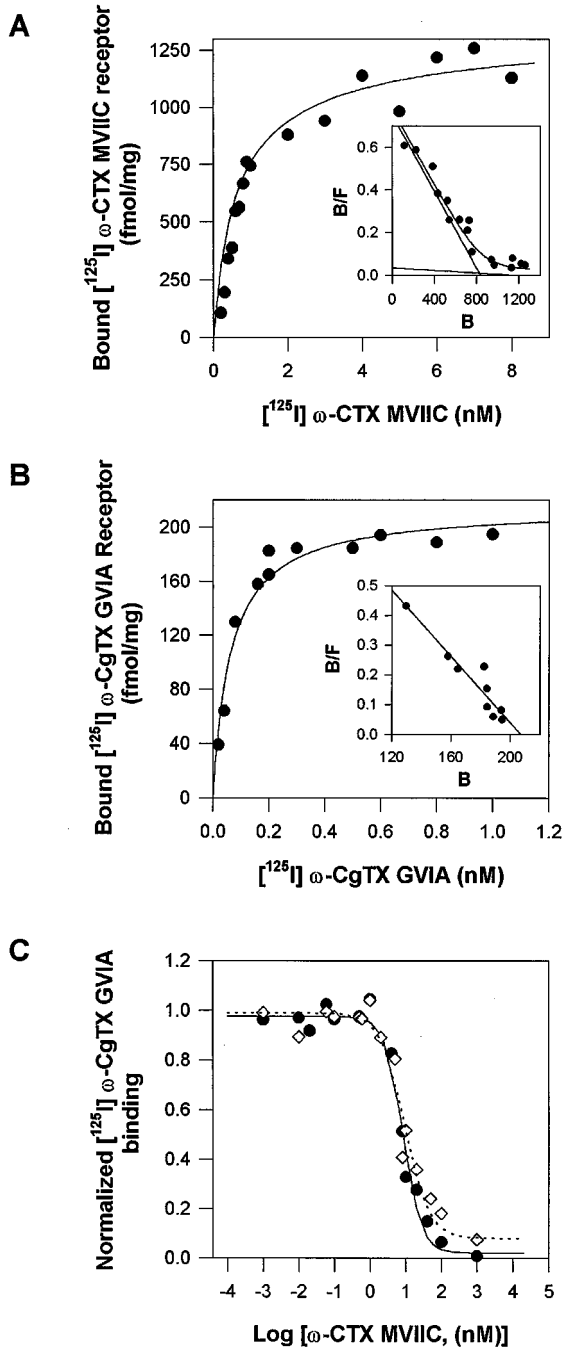

FIG. 1. **Binding of ^{125}I-ω-CTX MVIIC and ^{125}I-ω-CgTX GVIA to rabbit brain membranes.** *A*, direct binding curve and Scatchard analysis of ^{125}I-ω-CTX MVIIC binding to the rabbit brain membranes. Shown, receptor bound ^{125}I-labeled toxin (*B*) and free ^{125}I-labeled toxin (*F*). Two asymptotes of the hyperbola Scatchard plot (32) which represent two binding sites for ω-CTX MVIIC are shown in the insert. *B*, saturation curve and Scatchard analysis of ^{125}I-ω-CgTX GVIA binding to the rabbit brain membranes. Only one binding site can be detected for ω-CgTX GVIA. *C*, competition curve of ^{125}I-ω-CgTX GVIA binding to brain membranes (*dotted line, open diamond*) and solubilized brain extracts (*solid line, filled circle*) by unlabeled ω-CTX MVIIC. Data were normalized to the ^{125}I-ω-CgTX GVIA binding in the absence of ω-CTX MVIIC (100%). Analysis of data as given under "Experimental Procedures."

To establish which β subunit is associated with the α_{1A} pore-forming component of Ca^{2+} channel, we have produced β

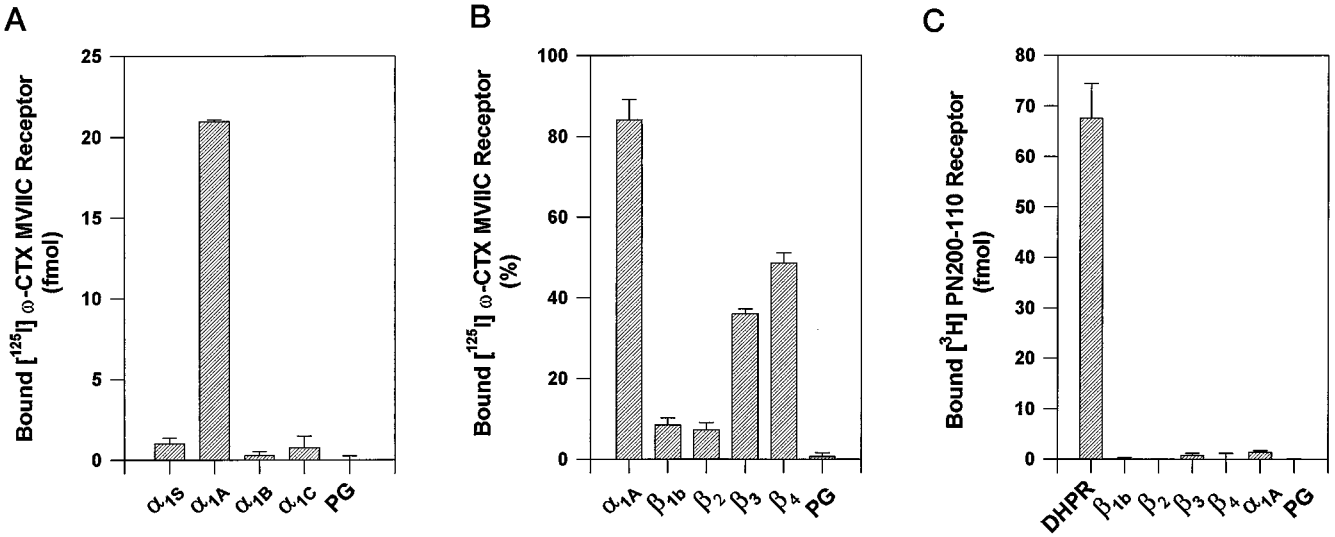

FIG. 2. **Immunoprecipitation of the high affinity ω-CTX MVIIC receptor and skeletal muscle L-type Ca^{2+} channel.** *A*, α_{1S}, α_{1A}, α_{1B}, and α_{1C} subunit antibodies were used to immunoprecipitate the high affinity ω-CTX MVIIC receptor. *PG* stands for protein G-Sepharose beads used as a negative control. *B*, immunoprecipitation of ^{125}I-labeled high affinity ω-CTX MVIIC receptor by α_{1A}, β_{1b}, β_2, β_3, and β_4 subunit antibodies. *C*, immunoprecipitation of ^{3}H-PN200–110-labeled skeletal muscle L-type Ca^{2+} channels by α_{1A}, β_{1b}, β_2, β_3, and β_4 subunit antibodies. DHPR stands for the polyclonal sheep antibody against skeletal muscle dihydropyridine receptor.

subunit subtype specific antibodies. β subunit genes have two highly homologous central domains, but unique N and C termini (Fig. 3*A*). Although domains I and II of each β subunit share 65 and 78% amino acid identity, respectively, the C termini of all four brain β subunits share only 3% amino acid identity. The C-terminal regions of four β subunits were thus expressed as GST fusion proteins. Excluding the common GST portion of these fusion proteins, the overall amino acid identity of all four fusion proteins is 1.2%. Antibodies were therefore raised against these fusion proteins in order to produce specific antibodies for each β subunit. As shown in Fig. 3*B*, the purified β_{1b}, β_2, β_3, and β_4 GST fusion proteins are of molecular mass of 52, 42, 39, and 34 kDa, respectively. The purified fusion proteins were used to generate polyclonal antibodies in rabbits (β_{1b}, β_2, and β_4) or sheep (β_3).

The specificity of each of the four FP antibodies was analyzed by immunoblotting. Crude bacterial lysates expressing the four fusion proteins were loaded on SDS-polyacrylamide gel electrophoresis. Approximately equal amounts of FPβ_{1b}, FPβ_2, FPβ_3, and FPβ_4 were present on the blots as determined by densitometry (corresponding Coomassie Blue-stained gel not shown). Since all four fusion protein antibodies should also contain antibodies against GST, they were removed by preincubation with bacterial GST lysates. Since an excess of fusion proteins were present in the blots, this assay should be very sensitive to detect any cross reactivity of the antibodies. As shown in Fig. 3*C*, antibodies to FPβ_{1b}, FPβ_2, FPβ_3, and FPβ_4 specifically recognized unique antigens and did not cross react with any of the other three fusion proteins in immunoblots. The antibodies to FPβ_{1b}, FPβ_3, and FPβ_4 also detected proteolyzed forms of the fusion proteins which were present in low amounts during the production of the fusion proteins.

In addition, the specificity of these antibodies for immunoprecipitation were tested using full-length *in vitro* translated β_{1b}, β_2, β_3, and β_4 subunits. ^{35}S-Labeled β_{1b}, β_2, β_3, and β_4 subunits were previously shown to be the only radiolabeled proteins present in the translation products (30). The results show that each antibody was able to immunoprecipitate their respective labeled β subunit but did not cross react significantly with the other three *in vitro* translated β subunits (Fig. 3*D*).

Immunoprecipitation of ^{125}I-ω-CTX MVIIC labeled high affinity receptors with the four β subunit specific antibodies was performed (Fig. 2*B*). β_4 immunoprecipitated the maximum amounts (48%) of bound receptor followed by β_3 36%, β_{1b} 8.4%, and β_2 7.2%. The results demonstrate that four different β subunits are present in high affinity ω-CTX MVIIC receptors. In contrast, none of the α_{1A} or four brain β subunit antibodies were capable of immunoprecipitating the skeletal muscle L-type Ca^{2+} channel (Fig. 2*C*). The C-terminal regions of brain β_{1b}, β_2, β_3, and β_4 subunits share little homology with the β_{1a} subunit of skeletal muscle L-type Ca^{2+} channels. The results suggest that none of these antibodies (β_{1b}, β_2, β_3, and β_4) reacted with the β_{1a} subunit of skeletal muscle L-type Ca^{2+} channel. The results also confirm that the nonspecific immunoprecipitation by each of these antibodies is negligible.

Copurification of α_{1A}, $\alpha_2\delta$, and Any One of the β_{1b}, β_2, β_3, and β_4 Subunits—The α_{1A} subunit antibody was raised against a 200-amino acid region, which is located on the cytoplasmic loop between domains II and III of the rabbit α_{1A} subunit. This region of α_{1A} shares a 37-amino acid sequence homology with the α_{1B} subunit, but shares little sequence homology with either α_{1S}, α_{1C}, α_{1D}, or α_{1E}. After enrichment of the Ca^{2+} channels on a heparin agarose column (26, 28), we utilized the mAb CC18 which was raised against the II-III loop of the α_{1B} subunit as an immunoaffinity ligand to specifically remove all the N-type Ca^{2+} channel (6), and then subsequently used an α_{1A} antibody affinity column to enrich the high affinity ω-CTX MVIIC receptor. The void from the mAb α_{1B} column was devoid of ^{125}I-ω-CgTX GVIA binding, showing that over 95% of the N-type Ca^{2+} channel was removed by mAb α_{1B} column (Fig. 4*A*). Second incubation with mAb α_{1B} column did not remove any additional ω-CgTX GVIA binding. Notably, the mAb α_{1B} column did not remove any ω-CTX MVIIC binding when brain receptors were labeled with 0.1 nM (data not shown) and 0.5 nM ω-CTX MVIIC, which only labeled the high affinity receptor as previously shown in Fig. 1*C*. In contrast, α_{1A} antibody affinity column bound greater than 95% of the labeled ω-CTX MVIIC receptor from the α_{1B} column void. The results demonstrate that the α_{1A} subunit is a major, if not the only, α_1 present in the high affinity ω-CTX MVIIC receptor. Since the eluted receptors were inactive in ω-CTX MVIIC binding, the enrichment of receptor could not be estimated. The recovery of protein from the α_{1A} column was about 0.3% compared to the total amount

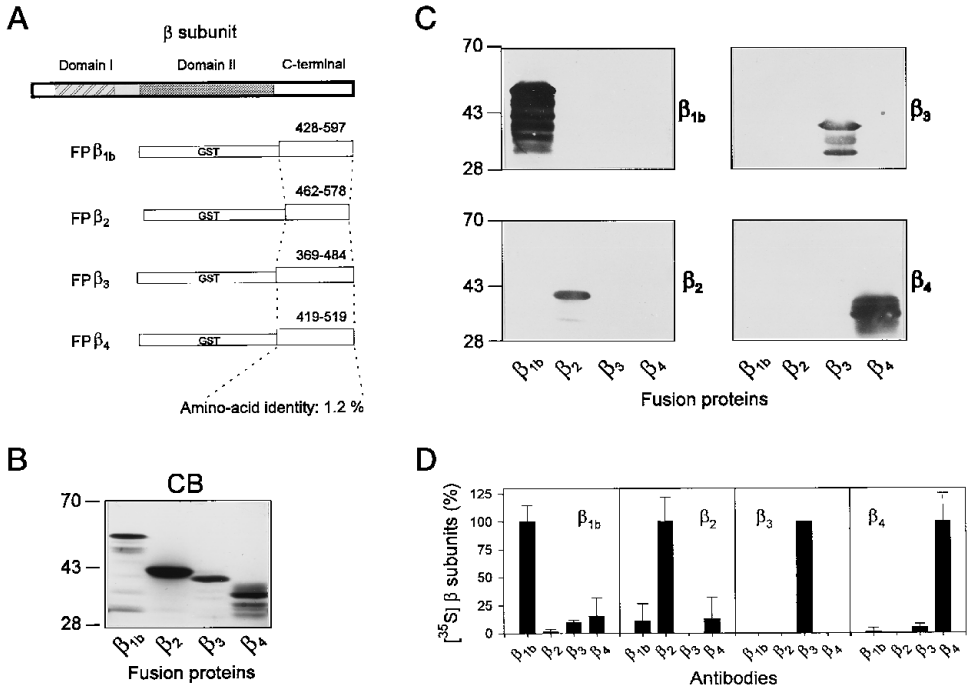

FIG. 3. **Production of β subunit subtype specific antibodies.** *A*, schematic representation of four fusion proteins containing GST polypeptide and C-terminal β subunits. All known β subunits have two highly homologous domains, *Domains I* and *II*. The numbers above the fusion protein inserts are the amino acid positions of each inserted β subunits. *B*, Coomassie Blue-stained SDS-polyacrylamide gel of four purified fusion proteins of C-terminal β subunits. Molecular mass markers (in kilodaltons) are on the *left*. These purified fusion proteins were used to produce β subunit antibodies. *C*, immunoblots stained with β subunit antibodies preadsorbed with GST bacterial lysates. The antibody used is shown on the right side of each immunoblot. *D*, immunoprecipitation of ^{35}S-labeled full-length β_{1b}, β_2, β_3, and β_4 subunits (marked inside each gragh) with four β subunit antibodies. Data were normalized by setting the value of the maximum immunoprecipitating antibody as 100% (n = 3).

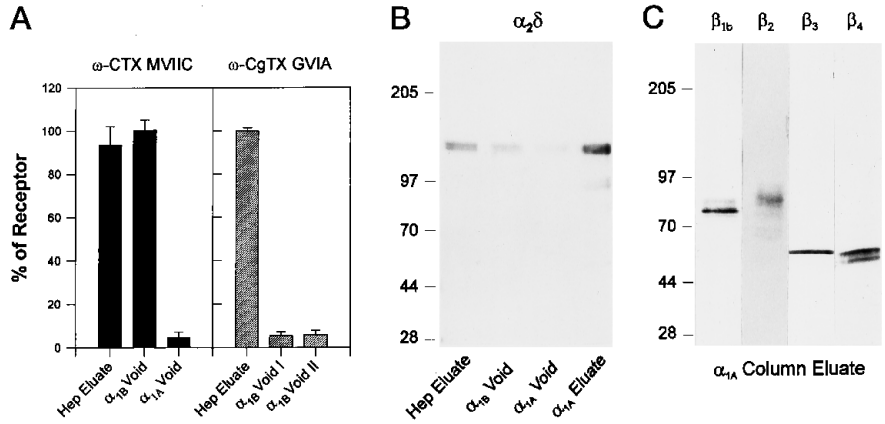

FIG. 4. **Partial purification of high affinity ω-CTX MVIIC receptors.** *A*, binding of 0.5 nM ^{125}I-ω-CTX MVIIC (*black bar*) or 0.5 nM ^{125}I-ω-CgTX GVIA (*shaded bar*) to solubilized rabbit brain receptors after elution from heparin (*Hep*) column, and passage through column of α_{1B} antibody, followed by α_{1A} antibody column or a second column of α_{1B} antibody. Equal amounts of total proteins (50 μg) were present in each condition. *B* and *C*, immunoblot analysis of enriched high affinity ω-CTX MVIIC receptor. Affinity purified antibodies against $\alpha_2\delta$ (*B*), β_{1b}, β_2, β_3, and β_4 subunits (*C*) were used. 100 μg of total proteins were present in heparin (*Hep*) eluate, α_{1B} column void and α_{1A} column void. Between 20–40 μg of total proteins were present in the α_{1A} column eluate, which is one-fourth of total eluted material from α_{1A} column with a starting 1-g brain membrane. Molecular mass markers (in kilodaltons) are on the *left*.

of protein loaded to the column (the α_{1B} column void) and about 0.02% compared to the quantity of starting brain membranes.

Further analysis of heparin column eluate, α_{1B} column void, α_{1A} column void and α_{1A} column eluate by immunoblotting showed that α_{1A}, $\alpha_2\delta$, β_{1b}, β_2, β_3, and β_4 subunits copurified on the α_{1A} immunoaffinity column. As shown in Fig. 4*B*, a fraction of the $\alpha_2\delta$ subunit was removed by the α_{1B} column since this subunit is also present in the N-type Ca^{2+} channel. Importantly, the α_{1A} column further removed another portion of the $\alpha_2\delta$ subunit and thus this subunit was enriched in the α_{1A} eluate. These results demonstrate that the $\alpha_2\delta$ subunit is also a component of the high affinity ω-CTX MVIIC receptor. In agreement with this result, wheat germ agglutinin-Sepharose sedimented a significant amount of high affinity ^{125}I-ω-CTX MVIIC receptors probably through its interaction with the heavily glycosylated $\alpha_2\delta$ subunit (data not shown). Similar to $\alpha_2\delta$ subunit, β_{1b}, β_2, β_3, and β_4 subunits were also enriched in the eluate of α_{1A} column (Fig. 4*C*) while they were barely detectable in 100 μg of α_{1B} column void (data not shown). The β_{1b} subunit has a molecular mass of 76 kDa on immunoblot. There is also a higher band running at 80 kDa which may be a modified form or a β_1 isoform. The β_2 subunit has a molecular

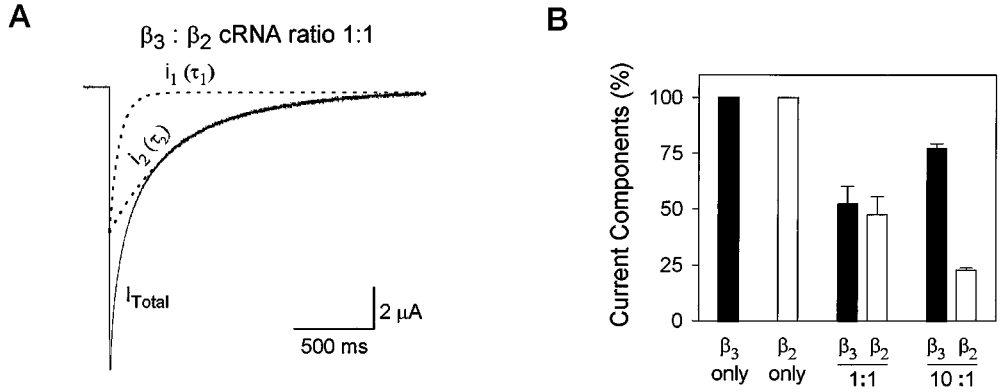

FIG. 5. **Coexpression of β_3 and β_2 subunits with the α_{1A} subunit in *Xenopus* oocytes.** *A*, trace example at 10 mV test potential and decomposition of the biphasic inactivating current into two components (*dashed line*). I_{Total} is the sum of i_1 and i_2 which represent two monophasic inactivating components. The time constants of these inactivation components are τ_1 = 62.8 ms and τ_2 = 454 ms. *B*, average percentage (i/I) of maximum current amplitude of α_{1A} $\alpha_2\delta_b$ β_3 and α_{1A} $\alpha_2\delta_b$ β_{2a} channels as inferred from the fits of the inactivation phase for β_3 only, β_2 only, and β_3:β_{2a} at cRNA ratios of 1:1 (n = 5) or 10:1 (n = 4). The *black bar* represents the β_3 component and *white bar* the β_{2a} component.

mass of 84 kDa. The β_3 subunit has a molecular mass of 58 kDa. The β_4 subunits appear to run at 59 and 55 kDa possibly representing differential phosphorylation states or isoforms. These results confirm the immunoprecipitation data with the β subunit antibodies. Furthermore, they demonstrate the specificity of β subunit antibodies on the immunoblot and the copurification of the $\alpha_2\delta$ and four β subunits during enrichment of high affinity ω-CTX MVIIC receptors.

Association of Various β Subunits with the α_{1A} Channel Contributes to Its Functional Diversity—Previously all four β subunits have been coexpressed separately with the α_{1A} and $\alpha_2\delta$ subunit in *Xenopus* oocytes. This results in several different modifications of the biophysical properties of the α_{1A} channel (10, 23). Previous results from our laboratory indicate that the current decay of the $\alpha_{1A}\alpha_2\delta$ channel coexpressed with the β_3 subunit is monophasic and fast (10), which resembles the Q-type current found in cerebellar granule cells (22). The current inactivation is voltage-dependent but reaches its fastest decay at +10 mV with a time constant of ~120 ms (10). When this channel is coexpressed with β_2 subunit, the current is slowly inactivating with a time constant of ~500 ms (10), which resembles the P-type current detected in cerebellar Purkinje cells (20).

Since an 18-amino acid domain in α_1 subunit has been identified to be responsible for β subunit association (36), the affinity of various β subunits binding to α_{1A} interaction domain has been determined (30). Compared to β_{1b}, β_2 and β_4 subunits, β_3 has a 10-fold lower affinity for α_{1A} interaction domain based on *in vitro* binding assay. To test if β_3 subunit is able to form Q-like channels in the presence of other β subunits in one cell, we coexpressed β_3 subunit with the β_2 subunit. The formation of $\alpha_{1A}\alpha_2\delta\beta_3$ or $\alpha_{1A}\alpha_2\delta\beta_2$ channel can be easily distinguished because these channels exhibit distinct inactivation kinetics. When β_3 and β_2 subunits were coexpressed in *Xenopus* oocytes with cRNA ratio of 1:1, the kinetics of the α_{1A} channel current showed a biexponential decay (Fig. 5*A*). The biphasic decay can be separated into two components with distinct inactivation kinetics (τ_1 = 69 ± 12 ms, τ_2 = 471 ± 32 ms, n = 5) which represents the currents carried by $\alpha_{1A}\alpha_2\delta\beta_3$ or $\alpha_{1A}\alpha_2\delta\beta_2$ channel. The results suggest the formation of two populations of functionally distinct channels. When β_3 and β_2 subunits were coexpressed in *Xenopus* oocytes with cRNA ratio of 10:1, the inactivation of the α_{1A} channel is also biphasic with a τ_1 of 59 ± 7 ms and a τ_2 of 338 ± 25 ms (n = 4). As expected for the formation of two populations of Ca^{2+} channel complexes, the time constants of the biphasic decay for both cRNA ratios were comparable to that of β_3 and β_2 expressed separately. While the total biexponential current is the sum of the two monoexponential components, the fast component (β_3) increased from 52 to 77% of the total current when cRNA ratio of β_3:β_2 changed from 1:1 to 10:1 (Fig. 5*B*). Although protein levels of β_3 and β_2 subunits could not be determined due to extremely low amounts of expression, these results show that both β_3 and β_2 subunits are able to associate with $\alpha_{1A}\alpha_2\delta$ to form functionally distinct channels for both β_3:β_2 cRNA ratios. Furthermore, these results suggest that the expression level of a β subunit may be one factor involved in α_{1A}·β complex formation.

DISCUSSION

There has been some controversy concerning the specificity of ω-CTX MVIIC in the literature. While some researchers found that this toxin blocks N-, P-, and Q- type Ca^{2+} channels (24, 25), others obtained specific blockage of P- and Q- type Ca^{2+} channels but not the N-type channel (19, 37). In this study, we detected both a high affinity and a low affinity binding site for this toxin in rabbit brain. Importantly, there is a critical concentration of ω-CTX MVIIC, below which the toxin specifically binds the high affinity receptor and above which the toxin starts to bind the N-type Ca^{2+} channel. Kristipati *et al.* (34) has reported that ω-CTX MVIIC binding is sensitive to concentration changes of monovalent (sodium, potassium) and divalent ions (calcium, barium) commonly used in biochemical and electrophysiological studies. It is conceivable that this critical concentration varies depending on the experimental conditions and different investigators were using variable ranges of the ω-CTX MVIIC concentration, which may explain some of the reported inconsistencies.

Although N-, P-, and Q-type Ca^{2+} channels are all involved in neurotransmission, P- and Q-type channels seem to be of greater importance than N-type not only in terms of larger Ca^{2+} currents but also in the efficacy of these Ca^{2+} currents coupling to neurotransmitter release (4, 22, 25, 38). The high affinity ω-CTX MVIIC receptor is expressed at a higher level than N-type channel which is in agreement with larger current expression of P- and Q-type channels. ω-CTX MVIIC has been used as a potent blocker for P- and Q-type Ca^{2+} channels (19, 22). Therefore the high affinity ω-CTX MVIIC receptor we detected in this study probably represents P- and Q-type Ca^{2+} channels.

Although it has been generally assumed that α_1, $\alpha_2\delta$, and β subunits may be common subunits for high voltage-activated Ca^{2+} channels, whether or not this holds true for all high voltage-activated channels has not been tested. Among the voltage-dependent Ca^{2+} channels, subunit composition of skel-

etal muscle L-type, cardiac muscle L-type and brain N-type channels have been extensively characterized, while brain L-type (α_{1C}- or α_{1D}-containing), P-type, Q-type, and α_{1E}-containing Ca^{2+} channels are poorly understood. Our data demonstrate for the first time that the high affinity ω-CTX MVIIC receptor is composed of at least an α_{1A}, $\alpha_2\delta$, and any one of the four β subunits. Furthermore, we demonstrate that different β-subunits are associated with the high affinity ω-CTX MVIIC-sensitive Ca^{2+} channel. This heterogenous association of β subunits results in channels with distinct properties such as inactivation kinetics when studied in *Xenopus* oocytes. Therefore, the association of various β subunits with the α_{1A} subunit in brain may produce some of the functional heterogeneity expected of Ca^{2+} channels sensitive to ω-CTX MVIIC.

The distinction between P- and Q-type Ca^{2+} channels is poorly defined. To our knowledge, there is no evidence to suggest that ω-CTX MVIIC has different affinity for brain P- or Q-type Ca^{2+} channels. The difference between inactivation kinetics of these channels could result from association of distinct β subunits. The only other known difference between these two channels are their sensitivity to ω-agatoxin IVA. Unfortunately, we and other investigators have found it difficult to obtain active radiolabeled ω-agatoxin IVA for biochemical studies. Based on our results, we propose that the high affinity ω-CTX MVIIC receptor represents both P-type and Q-type Ca^{2+} channel. It is likely that the combinations of various splice variants of α_{1A}, $\alpha_2\delta$, and their association with different β subunits may underlie the functional differences between P-type and Q-type Ca^{2+} channels. In support of this speculation, P-type represents the majority of Ca^{2+} channel current in cerebellar Purkinje cells where α_{1A} transcripts are most prominent (12, 23, 39). In our study, the α_{1A} subunit is the major (>90%) if not the only α_1 subunit of the high affinity ω-CTX MVIIC receptors. Since no gene other than the one encoding the α_{1A} subunit has been shown to encode a high affinity ω-CTX MVIIC receptor (21, 23), it is therefore possible that both P- and Q-type Ca^{2+} channels are encoded by splice variants of the α_{1A} gene.

Our data demonstrate that the high affinity ω-CTX MVIIC receptors in rabbit brain contain a diversity of β subunits in the following rank order, $\beta_4 > \beta_3 \gg \beta_{1b} \geq \beta_2$. Expression studies in *Xenopus* oocytes show that β subunits are able to associate with the α_{1A} channel in the presence of other β subunits in a single cell, and the expression level of a β subunit may be one factor involved in α_{1A}·β complex formation. Previously, the affinity of different β subunits binding to the α_{1A} interaction domain (fusion protein) were determined in the order of $\beta_4 \approx \beta_{2a} \approx \beta_{1b} > \beta_3$ (30). The estimated protein levels of the β subunits in rabbit brain are $\beta_3 \approx \beta_4 \geq \beta_{1b} > \beta_2$ (40). These results suggest that the interaction of the α_{1A} and β subunits *in vivo* may be dependent upon the spatial and temporal expression of β subunits and the affinity of α_{1A}-β subunit interaction.

The association of various β subunits with the same α_1 subunit increases the heterogeneity of voltage-dependent Ca^{2+} channels which are important in carrying out diverse functions. This is the first report that the high affinity ω-CTX MVIIC receptors are composed of at least α_{1A}, $\alpha_2\delta$, and any one of the four brain β subunits. Heterogeneity of high affinity ω-CTX MVIIC receptors in brain provides a structural basis for the functionally distinct channels such as P- and Q-type channels. These functional differences are likely to be significant determinants of efficient synaptic transmission.

Acknowledgments—We thank Laszlo Nadasdi from Neurex Corporation for providing us the ω-conotoxin MVIIC. We thank David Venzke for excellent technical assistance and Dr. Ricardo Felix for reading of the manuscript.

REFERENCES

1. Zhang, J.-F., Randall, A. D., Ellinor, P. T., Horne, W. A., Sather, W. A., Tanabe, T., Schwarz, T. L., and Tsien, R. W. (1993) *Neuropharmacology* **32,** 1075–1088
2. Krizanova, O., Diebold, R., Lory, P., and Schwartz, A. (1993) *Circulation* **87,** Suppl. VII, 44–48
3. Gaur, S., Newcomb, R., Rivnay, B., Bell, J. R., Yamashiro, D., Ramachandran, J., and Miljanich, G. P. (1994) *Neuropharmacology* **33,** 1211–1219
4. Castillo, P. E., Weisskopf, M. G., and Nicoll, R. A. (1994) *Neuron* **12,** 261–269
5. Witcher, D. R., De Waard, M., Sakamoto, J., Franzini-Armstrong, C., Pragnell, M., Kahl, S. D., and Campbell, K. P. (1993) *Science* **261,** 486–489
6. Scott, V. E. S., De Waard, M., Liu, H., Gurnett, C. A., Venzke, D. P., Lennon, V. A., and Campbell, K. P. (1996) *J. Biol. Chem.* **271,** 3207–3212
7. Catterall, W. A., and Streissnig, J. (1992) *Trends Pharmacol. Sci.* **13,** 256–262
8. Castellano, A., Wei, X., Birnbaumer, L., and Perez-Reyes, E. (1993) *J. Biol. Chem.* **268,** 3450–3455
9. Castellano, A., Wei, X., Birnbaumer, L., and Perez-Reyes, E. (1993) *J. Biol. Chem.* **268,** 12359–12366
10. De Waard, M., and Campbell, K. P. (1995) *J. Physiol.* **485,** 619–634
11. Jay, S. D., Sharp, A. H., Kahl, S. D., Vedvick, T. S., Harpold, M. M., and Campbell, K. P. (1991) *J. Biol. Chem.* **266,** 3287–3293
12. Mori, Y., Friedrich, T., Kim, M.-S., Mikami, A., Nakai, J., Ruth, P., Bosse, E., Hofmann, F., Flockerzi, V., Furuichi, T., Mikoshiba, K., Imoto, K., Tanabe, T., and Numa, S. (1991) *Nature* **350,** 398–402
13. Ellis, S. B., Williams, M. E., Ways, N. R., Brenner, R., Sharp, A. H., Leung, A. T., Campbell, K. P., McKenna, E., Koch, W. J., Hui, A., Schwartz, A., and Harpold, M. M. (1988) *Science* **241,** 1661–1664
14. Snutch, T. P., Leonard, J. P., Gilbert, M., Lester, H. A., and Davidson, N. (1990) *Proc. Natl. Acad. Sci. U. S. A.* **87,** 3391–3395
15. Snutch, T. P., Tomlinson, W. J., Leonard, J. P., and Gilbert, M. M. (1991) *Neuron* **7,** 45–57
16. Hullin, R., Singer-Lahat, D., Freichel, M., Biel, M., Dascal, N., Hofmann, F., and Flockerzi, V. (1992) *EMBO J.* **11,** 885–890
17. Collin, T., Wang, J. J., Nargeot, J., and Schwartz, A. (1993) *Circ. Res.* **72,** 1337–1344
18. Brust, P. F., Simerson, S., McCue, A. F., Deal, C. R., Schoonmaker, S., Willams, M. E., Velicelebi, G., Johnson, E. C., Harpold, M. M., and Ellis, S. B. (1993) *Neuropharmacology* **32,** 1089–1102
19. Turner, T. J., and Dunlap, K. (1995) *Neuropharmacology* **34,** 1469–1478
20. Mintz, I. M., Adams, M. E., and Bean, B. P. (1992) *Neuron* **9,** 85–95
21. Olivera, B. M., Miljanich, G. P., Ramachandran, J., and Adams, M. E. (1994) *Annu. Rev. Biochem.* **63,** 823–867
22. Randall, A., and Tsien, R. W. (1995) *J. Neurosci.* **15,** 2995–3012
23. Stea, A., Tomlinson, W. J., Soong, T. W., Bourinet, E., Dubel, S. J., Vincent, S. R., and Snutch, T. P. (1994) *Proc. Natl. Acad. Sci. U. S. A.* **91,** 10576–10580
24. Hillyard, D. R., Monje, V. D., Mintz, I. M., Bean, B. P., Nadasdi, L., Ramachandran, J., Miljanich, G., Azimi-Zoonooz, A., McIntosh, J. M., Cruz, L. J., Imperial, J. S., and Olivera, B. M. (1992) *Neuron* **9,** 69–77
25. Magnelli, V., Pollo, A., Sher, E., and Carbone, E. (1995) *Eur. J. Physiol.* **429,** 762–771
26. Sakamoto, J., and Campbell, K. P. (1991) *J. Biol. Chem.* **266,** 18914–18919
27. Peterson, G. L. (1977) *Anal. Biochem.* **83,** 346–356
28. Witcher, D. R., De Waard, M., and Campbell, K. P. (1993) *Neuropharmacology* **32,** 1127–1140
29. Gurnett, C. A., Kahl, S. D., Anderson, R. D., and Campbell, K. P. (1995) *J. Biol. Chem.* **270,** 9035–9038
30. De Waard, M., Witcher, D. R., Pragnell, M., Liu, H., and Campbell, K. P. (1995) *J. Biol. Chem.* **270,** 12056–12064
31. Krystal, G. (1987) *Anal. Biochem.* **167,** 86–96
32. Feldman, H. A. (1972) *Anal. Biochem.* **48,** 317–338
33. Lennon, V. A., Kryzer, T. J., Griesmann, G. E., O'Suilleabhain, P. E., Windebank, A. J., Woppmann, A., Miljanich, G. P., and Lambert, E. H. (1995) *N. Engl. J. Med.* **332,** 1467–1474
34. Kristipati, R., Nadasdi, L., Tarczy-Hornoch, K., Lau, K., Miljanich, G. P., Ramachandran, J., and Bell, J. R. (1994) *Mol. Cell. Neurosci.* **5,** 219–228
35. Martin-Moutot, N., Leveque, C., Sato, K., Kato, R., Takahashi, M., and Seagar, M. (1995) *FEBS Lett.* **366,** 21–25
36. Pragnell, M., De Waard, M., Mori, Y., Tanabe, T., Snutch, T. P., and Campbell, K. P. (1994) *Nature* **368,** 67–70
37. Sugiura, Y., Woppmann, A., Miljanich, G. P., and Ko, C.-P. (1995) *J. Neurocytol.* **24,** 15–27
38. Mintz, I. M., Sabatini, B. L., and Regehr, W. G. (1995) *Neuron* **15,** 675–688
39. Mintz, I. M., Venema, V. J., Swiderek, K. M., Lee, T. D., Bean, B. P., and Adams, M. E. (1992) *Nature* **355,** 827–829
40. Witcher, D. R., De Waard, M., Liu, H., Pragnell, M., and Campbell, K. P. (1995) *J. Biol. Chem.* **270,** 18088–18093
41. Lennon, V. A., Zwizinski, C. W., Kryzer, T. J., Luoma, E., Griesmann, G. E., O'Suilleabhain, P. E., Campbell, K. P., and Lambert, E. H. (1995) *Soc. Neurosci. Abstr.* **21,** 1283